© 2018. Published by The Company of Biologists Ltd | Development (2018) 145, dev152488. doi:10.1242/dev.152488

RESEARCH ARTICLE

The heart tube forms and elongates through dynamic cell rearrangement coordinated with foregut extension

Hinako Kidokoro[1,2,3], Sayuri Yonei-Tamura[2], Koji Tamura[2], Gary C. Schoenwolf[1] and Yukio Saijoh[1,*]

ABSTRACT

In the initiation of cardiogenesis, the heart primordia transform from bilateral flat sheets of mesoderm into an elongated midline tube. Here, we discover that this rapid architectural change is driven by actomyosin-based oriented cell rearrangement and resulting dynamic tissue reshaping (convergent extension, CE). By labeling clusters of cells spanning the entire heart primordia, we show that the heart primordia converge toward the midline to form a narrow tube, while extending perpendicularly to rapidly lengthen it. Our data for the first time visualize the process of early heart tube formation from both the medial (second) and lateral (first) heart fields, revealing that both fields form the early heart tube by essentially the same mechanism. Additionally, the adjacent endoderm coordinately forms the foregut through previously unrecognized movements that parallel those of the heart mesoderm and elongates by CE. In conclusion, our data illustrate how initially two-dimensional flat primordia rapidly change their shapes and construct the three-dimensional morphology of emerging organs in coordination with neighboring morphogenesis.

KEY WORDS: Actomyosin, Cardiogenesis, Cell rearrangement, Convergent extension, Heart fields, Heart tube formation, Morphogenesis

INTRODUCTION

The vertebrate heart originates from paired, splanchnic mesodermal primordia that flank the midline of the embryo and are intimately associated ventrally with the endoderm. These primordia merge medially to form the heart tube, which then rapidly elongates anteroposteriorly. As the heart tube elongates, it undergoes looping, during which it is remodeled into the characteristic multi-chambered organ of vertebrates. Adequate elongation of the heart tube is essential for normal looping, as defects in elongation cause improper remodeling and cardiac malformations (Cai et al., 2003; Kelly and Buckingham, 2002; Lyons et al., 1995; Sinha et al., 2015; Tanaka et al., 1999).

Elongation of the heart tube was long believed to be due mainly to anterior-to-posterior fusion of the paired, elongated heart primordia in the midline (Fig. S1) (Abu-Issa and Kirby, 2007; DeHaan, 1965; Harvey, 1998). However, this view was challenged by the finding that the anterior pole of the heart tube is derived from the medial part of the bilateral heart primordia, areas collectively called the second heart field (SHF), as opposed to the first heart field (FHF), the lateral part of the primordia (Fig. 1A) (Cai et al., 2003; Kelly et al., 2001). Identification of the SHF has led to the notion that heart-tube elongation occurs by progressive addition of SHF cells to the poles of the FHF-derived initial heart tube. However, this idea has never been experimentally examined and how SHF cells are added remains unclear. Based on 3D reconstruction and labeling of the heart primordia, it was proposed that heart progenitor cells that form the successive anteroposterior levels of the whole heart tube are initially arrayed mediolaterally in the bilateral heart primordia (Fig. 1B) (Abu-Issa and Kirby, 2008). Thus, contrary to the previous belief (Fig. S1B), recent studies indicate that the long anteroposterior dimension of the elongated heart tube forms from the narrow mediolateral dimension of the oblong heart primordia (Fig. 1B) (Abu-Issa and Kirby, 2008; Kelly et al., 2001). This begs the question, what mechanism drives this dramatic morphological change (Fig. 1B) and results in rapid anteroposterior elongation of the heart tube?

During formation of the heart tube, the endoderm ventral to the heart primordia folds to form the tubular, midline foregut. Concomitant with this, the paired heart primordia pivot/fold toward the ventral midline, flipping and fusing to form the heart tube ventral to the newly formed foregut (Fig. S2A). As the anterior intestinal portal (AIP, the posterior opening of the foregut) descends posteriorly, the foregut and primitive heart tube elongate posteriorly together (Fig. S2B). Recent studies have suggested that the endoderm plays an active mechanical role in fusion of the paired heart primordia, pulling them toward the midline where they appose and fuse (Aleksandrova et al., 2015; Varner and Taber, 2012; Ye et al., 2015). In addition, a recent model proposes that endodermal myosin contraction around the AIP generates posteriorward forces that assist the elongation of the foregut and heart tube (Hosseini et al., 2017), but the extent to which movements of these two tissues are coordinated is unknown.

Using cell cluster labeling and live imaging, we show that the originally narrow mediolateral dimension of the heart primordia rapidly and directionally extends to generate the entire length of the early heart tube. This extension is accompanied by convergence in the perpendicular plane, i.e. along the initially long anteroposterior axis. Thus, the heart primordia dynamically change their morphology by convergent extension (CE), transforming into the long and narrow heart tube. We further demonstrate that CE is driven by oriented cell rearrangement that is dependent on actomyosin contraction. Finally, we find that the associated endoderm coordinately forms the foregut through previously unrecognized movements that parallel those of the heart mesoderm, also lengthening by CE.

RESULTS

Extensive labeling of heart mesoderm reveals tissue dynamics and cell movements during early heart tube formation

Although previous fate-mapping studies have greatly advanced our knowledge of heart tube formation, there are still enormous gaps in

[1]Department of Neurobiology and Anatomy, University of Utah School of Medicine, Salt Lake City, UT 84132-3401, USA. [2]Department of Developmental Biology and Neurosciences, Graduate School of Life Sciences, Tohoku University, Sendai, 980-8578, Japan. [3]Department of Cell Biology, National Cerebral and Cardiovascular Center Research Institute, Suita, Osaka 565-8565, Japan.

*Author for correspondence (yukio.saijoh@neuro.utah.edu)

Y.S., 0000-0002-7548-4789

Received 1 April 2017; Accepted 21 February 2018

Development (2018) 145, dev152488. doi:10.1242/dev.152488

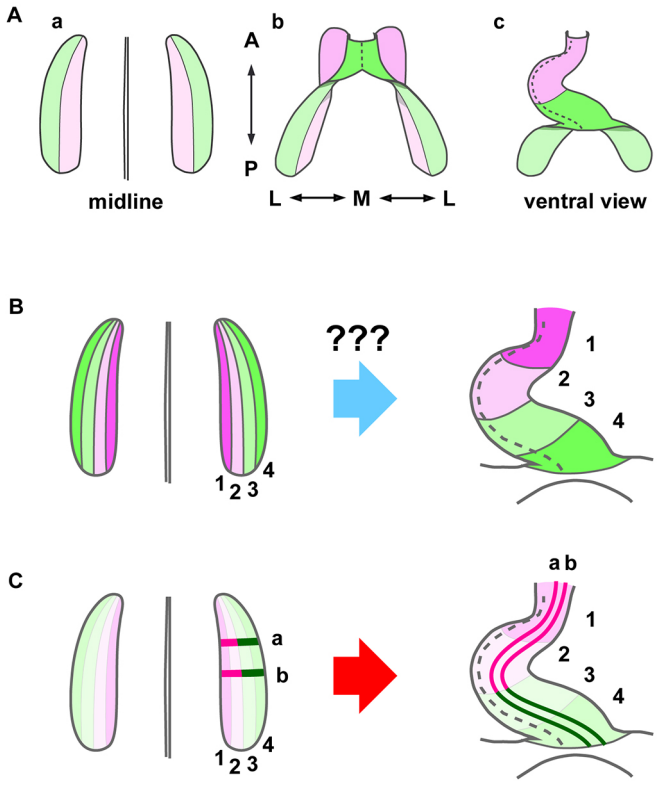

Fig. 1. Heart fate maps. (A) Kelly et al. (2001) have revealed that the progenitors that form the anterior region (pink) of the heart tube (Ac) originally reside in the medial part (pink) of the bilateral heart primordia (Aa), which is the so-called second heart field (SHF, pink), as opposed to the first heart field (FHF, green), the lateral part of the primordia. (B) Abu-Issa and Kirby (2008) proposed that the progenitors that form the corresponding anterior-to-posterior levels of the heart tube are initially organized in medial-to-lateral sequence in each heart primordium. However, how the primordia undergo such a dramatic morphogenetic rearrangement remains unknown (question marks). (C) Our new model based on cell cluster labeling data in this study (Figs 2 and 3) showing that the heart primordia undergo dynamic tissue reshaping through CE. Areas 1 (magenta) and 2 (pink) constitute the SHF and areas 3 (light green) and 4 (green) constitute the FHF. A, anterior (cranial); P, posterior (caudal); M, medial; L, lateral.

our understanding of the mechanisms shaping the early heart tube. To elucidate how the paired heart primordia transform their morphology into an elongated tube, we visualized tissue-scale dynamics during heart tube formation by labeling cell clusters in both the lateral and medial parts of the bilateral heart primordia (LHP and MHP, respectively). Although the regions termed LHP and MHP in this study approximate the so-called first and second heart fields (FHF and SHF), respectively (Buckingham et al., 2005), we mainly use LHP and MHP, as we analyzed their morphogenesis based on their relative positions within the embryo. Previous studies suggested that the LHP/FHF first merge to form the initial heart tube and, subsequently, that MHP/SHF cells are 'added' to the poles of the LHP/FHF-derived initial heart tube. This addition of MHP/SHF cells is considered crucial for heart tube elongation. However, how this occurs remained unclear (Francou et al., 2014; Kelly et al., 2001; Ma and Adelstein, 2012; Sinha et al., 2012, 2015; Uribe et al., 2014). To address this, we first labeled only the MHP by injecting the vital fluorescent dye, DiO, to mark stripes of cells at three anteroposterior levels, well before midline apposition and fusion of the paired primordia had occurred. Embryos were then subjected to time-lapse recording (Fig. 2, Movie 1).

Throughout the recordings, the three labeled cell stripes in each of the paired MHP moved synchronously (Fig. 2A-J, Movie 1), suggesting that the primordia move as cohesive cell sheets throughout early heart tube formation. In addition, these cell movements were highly coordinated with movements of the AIP (yellow lines in Fig. 2A′-J′), which converged medially while descending posteriorly, progressively extending the foregut posteriorly. At the three-somite stage (t0:00), the small foregut pocket (Fig. 2A′, arrowhead) was already formed at the cephalic (anterior) end of the embryo (Fig. 2A,A′). In concert with AIP convergence and descent, the labeled MHP ventrally folded diagonally toward the medial-posterior direction (Fig. 2A-E; Fig. 2B′, arrow; Fig. 7Aa-c; note that the cell streams, which are initially aligned mediolaterally, are now oriented diagonally along the anteroposterior axis). This diagonal folding is thought to be important for realigning the initial mediolateral polarity of the bilateral heart fields to the anterior-posterior direction (Abu-Issa and Kirby, 2008; Hosseini et al., 2017). The coordinated movements between the heart primordia and AIP suggest that diagonal folding of the heart primordia may be driven by medial convergence and posteriorward motion of the AIP (Fig. 2A′-E′). Interestingly, during folding, labeled cell clusters rapidly extended medioposteriorly towards the center of the AIP (Fig. 2D′-F′; Fig. 2D′, arrow), such that all stripes synchronously extended in tandem with AIP movement (Fig. 2D-F, Movie 1). When the leading cells (Fig. 2F′, blue dot) of the extending stripes neared the midline, the primitive, short (i.e. anteroposterior dimension) heart tube emerged (Fig. 2F,F′, white line), suggesting that the paired heart primordia partly merged at the midline. At this time, only the medial region (original lateral region before folding; Fig. 2F′, blue dot) of the stripes were contained within the heart tube proper, with the remainder occupying the continuous dorsal heart mesoderm on the left and right sides (Fig. 2F,F′, arrowheads; Fig. 7Ad). Subsequently, those stripes of cells in the dorsal heart mesoderm (Fig. 2F′, arrowheads) progressively merged toward the midline (Fig. 2G,G′, arrows), further reorienting the cell stream along the anteroposterior axis to incorporate into the forming anterior (arterial) pole of the heart tube (Fig. 2H-J,H′-J′), with the entire length of the stripes continuing to extend. Importantly, incorporation of the three cell stripes in each MHP (i.e. the three different anteroposterior labeled populations) into the heart pole occurred nearly synchronously (Fig. 2A-J, Movie 1), despite being originally widely separated (Fig. 2A,A′, asterisk). In addition, the distance between cell stripes decreased substantially during incorporation [compare distances between the stripes (asterisk) in Fig. 2A′ and J′, Fig. S3A,B]. Our observations suggest that the paired heart primordia were not just brought together in the midline for fusion, but rather that the primordia underwent active convergence at the tissue level, joining at the midline to form the narrow heart tube. Of note, while the distance decreased between stripes of labeled cells in each primordium, the stripes rapidly increased their length in the perpendicular direction (i.e. the primordia extended; Fig. 2D′, arrow) along the elongating axis of the heart tube (Fig. 2D-J). Collectively, these observations suggest that the MHP undergo convergent extension (CE) to form the narrow, elongated anterior heart tube.

In summary, our observations suggest that formation of the heart tube from the MHP is accomplished through three steps: (1) ventral folding of paired heart primordia diagonally toward the medial-posterior direction in concert with AIP convergence and descent (Fig. 7Aa-c), realigning the initial medial-lateral polarity along the anterior-posterior axis of the embryo; (2) progressive fusion of paired primordia at the midline, presumably seaming up the initial anterior edges of the paired MHP (Fig. 7Ac,d) (Abu-Issa and Kirby,

Development (2018) 145, dev152488. doi:10.1242/dev.152488

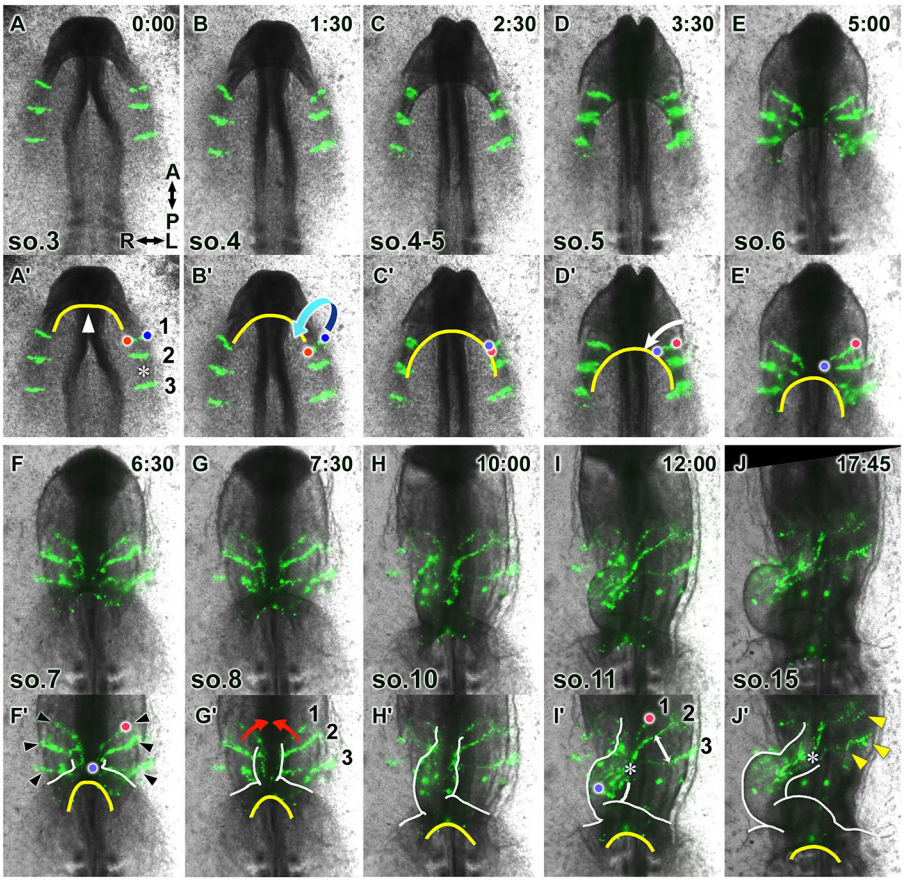

Fig. 2. The heart primordia undergo rapid directional extension while converging perpendicularly during heart tube formation. To visualize tissue dynamics during heart tube formation, the medial parts of the bilateral heart primordia (MHP) were labeled with DiO and imaged using epifluorescence time-lapse microscopy (Movie 1). (A-J) Selected images from the movie (ventral view), with relative times after the initiation of the recording (h:min) and somite stages indicated in the upper right and bottom left corners, respectively. (A′-J′) Annotated duplicate images. Red and blue dots in A′-F′,I′ depict the original medial and lateral edges, respectively, of the labeled cell stripe. In concert with the movement of the anterior intestinal portal (AIP, yellow lines), the paired heart primordia folded ventrally, diagonally in the medial-posterior direction (arrow, B′), reorienting the original transverse cell stripes longitudinally (C′-E′). During folding, each heart primordium extended medioposteriorly (arrow, D′), along with convergence and descent of the AIP. Subsequently, the paired primordia merged medially (red arrows, G′), further reorienting the cell streams to the anteroposterior direction. White lines in F′-J′ depict the outline of the heart tube. The distance between labeled cell stripes (asterisk in A′) decreased after the heart tube formed (asterisk in I′,J′), whereas the cell stripes, which had not yet incorporated into the heart tube, remained separated (double-headed arrow in I′). At the end time-point, some MHP-derived labeled cells remained in the dorsal heart mesoderm (arrowheads in J′) in continuity with the labeled cell stripes within the anterior heart tube.

2008); and (3) convergence of the primordia along the original anterior-posterior axis during folding (1) and fusion (2). As the anterior-posterior axis reorients to the medial-lateral direction by diagonal folding (1) and subsequent fusion (2), the paired heart primordia actually converge toward the midline, transforming the flat primordia into a narrow midline tube. Convergence is accompanied by extension along the perpendicular direction, i.e. along the rapidly elongating axis of the heart tube.

Thus, although MHP cells are generally assumed to incorporate into the heart tube in a manner different from that of the LHP, our data show that the MHP form the early heart tube in basically the same way as do the LHP, by folding and merging at the midline. In addition, our data suggest that CE propels transformation of the flat heart primordia into the midline tube by converging them toward the midline, while extending them perpendicularly to generate the rapidly elongating heart tube.

The narrow mediolateral dimension of the heart primordia gives rise to the entire length of the elongated early heart tube

Labeled MHP cells contributed to only the anterior region of the heart tube (Fig. 2J,J′) (Abu-Issa and Kirby, 2008; Cai et al., 2003; Kelly et al., 2001), which forms the future right ventricle and outflow tract (Männer, 2000, 2009). We next labeled both the MHP and LHP in various patterns to establish how cells within the bilateral heart primordia change their relative positions during heart tube formation.

First, we labeled MHP and LHP with DiI (magenta) and DiO (green), respectively (Fig. 3A, Movie 2). This pattern of labeling allowed clear visualization of how the initial mediolateral organization of the heart primordium changes to anteroposterior organization in the heart tube (Abu-Issa and Kirby, 2008; Cai et al., 2003; Kelly et al., 2001). In tandem with AIP convergence and descent, the MHP (magenta) first folded ventrally in the medioposterior direction (Fig. 3Aa-e; where the signal appears white, magenta cells overlap, i.e. lie dorsal to, green cells as the rudiments fold; Fig. 7Ba,b, Fig. S4). This diagonal folding of the MHP brought the LHP (green) medioposteriorly toward the midline, and the first fusion of the paired primordia occurred near the MHP and LHP boundary (Figs 3Aa-f and 7Ba-c). At this time, the LHP has not yet folded. As the AIP further descended, the paired LHP folded medioposteriorly in the wake of the previously folded MHP (Fig. 3Af-h). Thus, both the MHP and LHP folded medioposteriorly in coordination with AIP convergence and descent. Owing to differences in their position with respect to the AIP, folding occurred progressively from the medial (MHP) to lateral (LHP) sides of the primordium (Fig. 7B,C), suggesting that diagonal folding of the heart primordia is directed by AIP movements. While folding, the paired LHP progressively fused at the midline from their original medial side to form the posterior part of the heart tube (Fig. 3Af-h). Concomitantly, the MHP formed the anterior part of the heart tube, but because folding of the paired MHP was already completed, they simply fused toward the midline from their original lateral side, with the labeled cell stripes progressively merging medially and incorporating into the nascent arterial (anterior) pole of the heart tube (Figs 3Af-h and 7Bc,d, Movie 2). Thus, the initial midline fusion of the paired heart primordia occurred near the original boundary between the MHP and LHP, and progressed bidirectionally, zipping up the MHP and LHP in anterior and posterior directions, respectively (Fig. 3Af-h, Movie 2, Fig. 7B) (Moreno-Rodriguez et al., 2006).

Development (2018) 145, dev152488. doi:10.1242/dev.152488

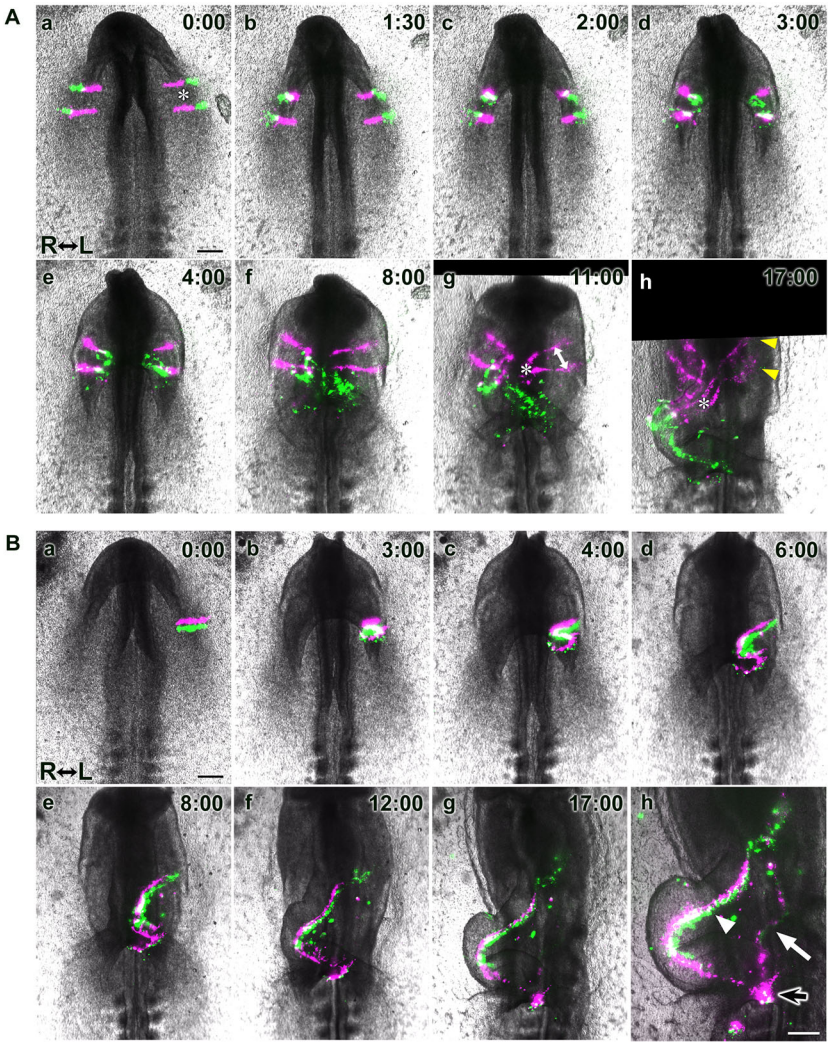

Fig. 3. The bilateral heart primordia reorient during heart tube formation. (A,B) Selected images from time-lapse recordings (Movies S2 in A and S3 in B). (Aa-h) The medial (magenta) and lateral (green) parts of the heart primordia (MHP and LHP) were labeled with DiI and DiO, respectively. Both the MHP (magenta) and LHP (green) directionally extended, giving rise to the entire length of the early heart tube, with each primordium contributing the anterior and posterior regions of the tube, respectively. The distance between adjacent stripes in the same primordium substantially reduced during heart tube formation (compare the distances indicated by the asterisks in a and h, and the distances indicated by the double-headed arrow and asterisk in g). Yellow arrowheads in Ah indicate MHP-derived labeled cell populations that reside in the dorsal heart mesoderm. (Ba-h) Two stripes of cells at different anteroposterior levels in the left heart primordium were labeled with DiI (magenta, anterior) and DiO (green, posterior), respectively. Anteroposterior polarity in the heart fields reoriented into the mediolateral (ventrodorsal) polarity of the heart tube. (h) An image taken with a longer exposure time to detect fluorescent signals in the foregut (white arrow) and heart tube (arrowhead); the black arrow marks an area where labeled cells in both the heart tube and adjacent foregut overlap. Scale bars: 200 µm.

However, elongation of the heart tube was not due solely to the progression of fusion. Rather, labeled cell clusters in both the MHP (magenta) and LHP (green) rapidly and directionally extended during heart tube formation. As a result of directional extension, these originally medial and lateral cell populations formed single continuous streams, extending throughout the anteroposterior dimension of the early heart tube, with each cell population contributing to the anterior (magenta) and posterior (green) parts of the tube, respectively (Figs 3Aa-h and 1C). This result indicates that the short mediolateral dimension of the bilateral heart primordia directionally extends to give rise to the entire length of the early heart tube. Of note, directional extension of labeled cell clusters occurred in concert with AIP movements. Labeled cells in the LHP extended synchronously with AIP descent throughout the recording, whereas MHP showed such synchronized extension with AIP movements only at early stages, when the paired MHP folded medioposteriorly for fusion (Figs 3Aa-e and 2A-E). At later stages, the AIP further moved posteriorly and became distant from the MHP (Figs 3Af-h and 2F-J). Nevertheless, labeled cells in the MHP continued to extend, suggesting that extension of the MHP at these later stages is less dependent on AIP movements.

To visualize how the anteroposterior orientation of the heart primordia changes during heart tube formation, we next labeled two anteroposterior stripes of cells in the left heart primordium with DiI and DiO, respectively (Fig. 3B, Movie 3). As the heart tube formed, the anterior stripe (magenta) localized medial to the posterior stripe (green), consistent with the results shown in Figs 2 and 3A. Together, these data provide strong evidence that cells arrayed in an anteroposterior position in the bilateral heart primordia reorient to a mediolateral (ventrodorsal) position in the heart tube.

Labeled cell clusters in both the MHP and LHP always underwent a dramatic and directional extension (Figs 2 and 3A,B) during heart tube formation. Importantly, the distance between cell stripes decreased substantially, perpendicularly to the direction of extension [compare the distances between the stripes (asterisk) in Figs 2A′ and J′ and 3Aa and Ah, Fig. S3A,B]. This reduction was evident within the newly formed heart tube, whereas cell stripes in the dorsally contiguous heart mesoderm (dorsal heart mesoderm), which had not yet incorporated into the heart tube, remained separated (Fig. 2I′ and 3Ag, compare the distances indicated by the arrow and asterisk, Fig. S3C). Based on this, we hypothesized that the heart mesoderm undergoes CE to form the heart tube.

Heart mesoderm undergoes CE driven by cell-cell intercalation

To test this hypothesis, we asked whether heart mesodermal cells undergo cell-cell intercalation. We labeled two anteroposteriorly adjacent regions in the heart primordia, one with DiI (magenta) and the other with DiO (green), and imaged the labeled cells at cellular resolution with confocal microscopy. At the time of labeling, the

Development (2018) 145, dev152488. doi:10.1242/dev.152488

two stripes were completely separate from one another (Fig. 4Aa, Movie 4). After the heart tube formed (approximately 24 h later), the two stripes abutted one another, with green and red cells intermingled (Fig. 4b-b″, Movie 5, *n*=4). The myocardium at this stage consisted of two cell layers. Cells in both layers were preferentially elongated along the convergence axis (Fig. 4Ab,b′: outer layer, b″: inner layer), which is typical of intercalating cells. Thus, these data provide strong evidence that the heart mesoderm undergoes CE driven by cell-cell intercalation.

Directional cell-cell intercalation in heart mesoderm is myosin dependent

To ask whether actomyosin drives directional cell rearrangement in the heart mesoderm (Fig. 4Ab-b″), we first examined the distribution of active/phosphorylated non-muscle myosin II by detecting its phosphorylated myosin regulatory light chain (pMLC) (Ma and Adelstein, 2012) immunohistochemically. Phosphorylated-myosin II (p-myoII) localizes preferentially along the convergence axis and generates forces that drive tissue remodeling (Bertet et al., 2004; Kasza and Zallen, 2011; Nishimura et al., 2012; Rozbicki et al., 2015; Zallen and Wieschaus, 2004). Consistent with this, in the dorsal heart mesoderm, which subsequently incorporates into the heart tube, p-myoII was enriched in cellular junctions aligned perpendicularly to the direction of tissue extension, forming polarized myosin supracellular cables (Fig. 4Ba-b′, yellow arrows in Fig. 4Ba depict the direction of tissue extension observed in Fig. 2; Fig. S5). Next, we inhibited myosin contractility with Y27632, a Rho-associated protein kinase (ROCK) inhibitor; p-myoII localization at cellular junctions was abolished (Fig. 4Bc,c′). Finally, we labeled the heart mesoderm with DiI and treated embryos with Y27632 (Fig. 4C, Movie 6). Although the bilateral heart primordia folded and formed the heart tube, the labeled cell cluster failed to extend [almost no extension occurred in five out of seven embryos, with considerable reduction in extension in the remaining two, resulting in a striking shortening of the heart tube (*n*=7/7) compared with that of control embryos (*n*=3, Fig. S6)]. These results suggest that ROCK-dependent myosin contractility is crucial for driving directional rearrangement of heart cells/CE to lengthen the heart tube.

Foregut endoderm and heart mesoderm are intimately associated during heart tube formation and elongation

In our cell labeling experiments, we identified an additional stream of dye (Figs 3Bh and 5Bb, white arrows) that was faint and outside of the heart tube (Figs 3Bh and 5Bb, arrowheads). Apparently, injection

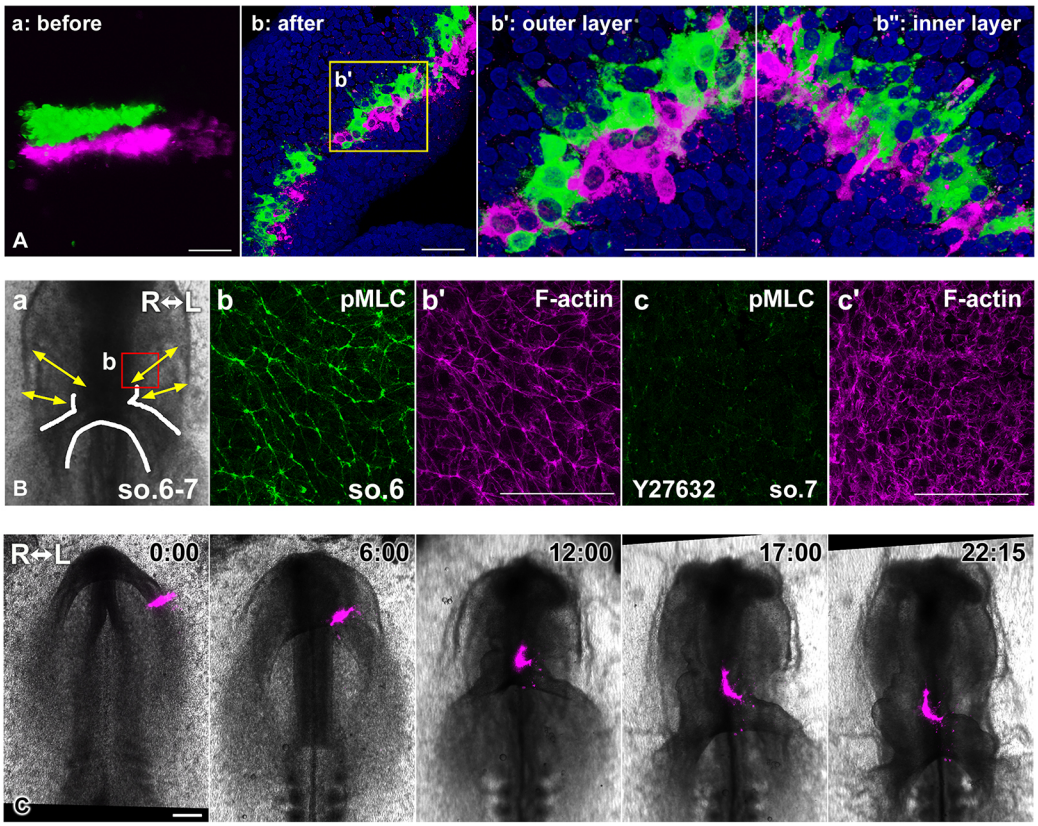

Fig. 4. Heart mesodermal cells undergo intercalation during heart tube formation. (A) Confocal images (3D rendering) of labeled cells in the heart mesoderm. (a) Two cell stripes in anteroposteriorly adjacent regions within one heart primordium were labeled with DiI (magenta) and DiO (green) prior to fusion of the paired primordia, and immediately imaged (a, Movie 4). (b-b″) After the heart tube formed, the DiI- and DiO-labeled cells were intermingled (Movie 5). (b′,b″) Enlargement of the region indicated by the box in b showing the exterior wall (b′) and interior wall (b″) of the myocardium. In both b′ and b″, myocardial cells exhibit a polarized, elongated shape, typical of intercalating cells. Scale bars: 50 µm. (B) The heart mesoderm was immunostained with anti-phosphorylated myosin light chain (pMLC) antibody (green, b,c) and counterstained with fluorescent-phalloidin to label F-actin (magenta, b′ and c′). (a) The box indicates the approximate area shown in b,b′ and c,c′. Arrows indicate the direction of heart mesoderm extension observed in our cell labeling (Fig. 2). The white line outlines the heart. (b-c′) Projections of confocal *z* stacks. (b,b′) Normal embryo at stage 9– (6-somite stage). In the dorsal heart mesoderm, phosphorylated-myosin (p-myoII) is enriched at cell junctions, which are aligned perpendicularly to the direction of tissue extension (arrows in a). (c,c′) Y27632-treated embryo at stage 9 (7-somite stage). p-myoII localization at cell junctions and the polarized distribution of F-actin are abolished. Scale bars: 50 µm. (C) Selected images from a time-lapse recording (Movie 6). Y27632 treatment blocked directional extension of the labeled cell cluster (magenta) in the heart mesoderm and heart tube elongation. Scale bar: 200 µm. All images except Ab″ (interior surface view of myocardial wall) are ventral views.

Development (2018) 145, dev152488. doi:10.1242/dev.152488

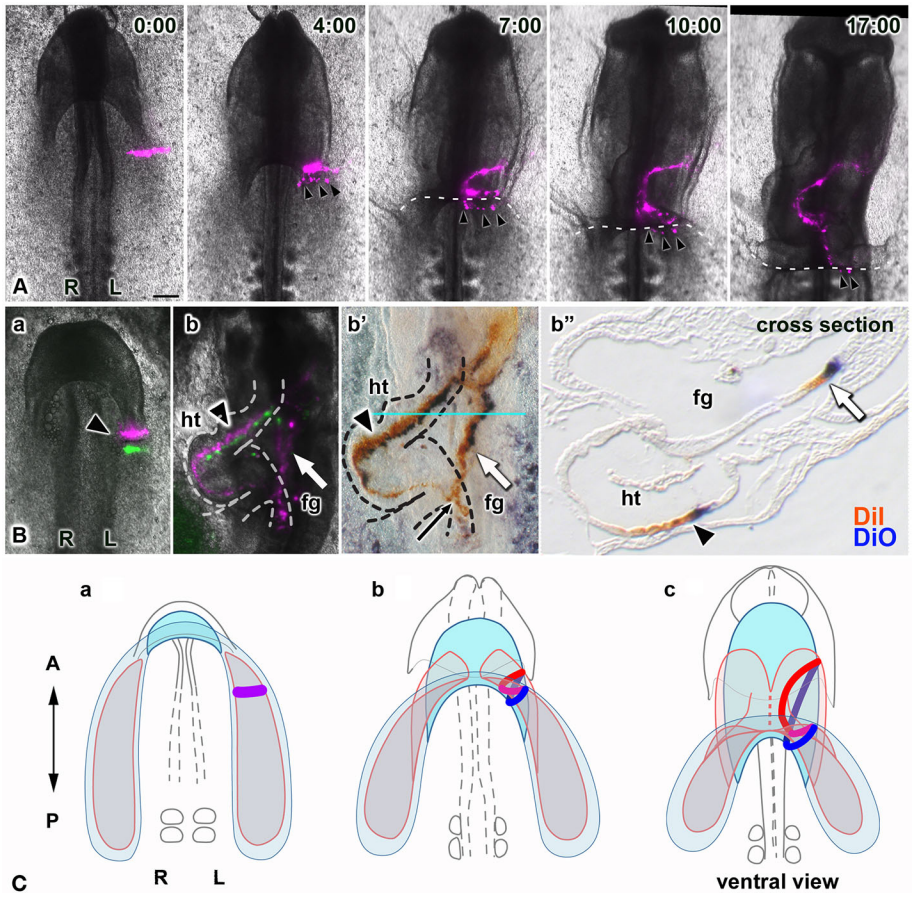

Fig. 5. The heart tube and foregut coordinately form and lengthen through similar tissue dynamics. (A) Selected images from a time-lapse recording (Movie 7, ventral views), showing movements of a single stripe of labeled cells (magenta) in one heart primordium along with endodermal cells (arrowheads), accidentally marked when DiI was injected into the heart mesoderm. Dashed lines delineate the edge of the LHP. Labeled endodermal cells roll over the AIP into the foregut as the AIP descends, concomitant with folding of the LHP, demonstrating that movements of these two primordia are coupled. Scale bar: 200 µm. (B) Two stripes of labeled cells (magenta, DiI and rhodamine, anterior stripe; green, DiO and fluorescein, posterior stripe) at the time of injection (a, arrowhead) and after heart tube formation (b, arrowhead). Dyes were then immunostained in whole-mount embryos (b′) to enhance and preserve their labeling (rhodamine, brown; fluorescein, dark blue) during subsequent paraffin sectioning (b″). Labeled cells extended anteroposteriorly in both the heart tube (ht; arrowheads) and foregut (fg; white arrow); the black arrow marks an area where labeled cells in the heart and foregut overlap. (b″) Paraffin wax-embedded cross-section at the level shown by the blue line in b′. (C) Model of coordinated formation of the foregut and heart tube based on our results (A,B): the endoderm (blue) overlying the bilateral heart primordia (pink) converges toward the midline while diagonally folding, thereby reorienting its initial mediolateral polarity anterorposteriorly, coordinately with heart tube formation. These tubes elongate posteriorly together through CE. The red and blue lines in b and c represent simultaneously labeled cell stripes (a, purple line) in the heart mesoderm and in the endoderm, respectively.

of dye into the heart mesoderm from the ventral side of the embryo accidentally also labeled the overlying endoderm, as those layers are in close contact at the stages injected. Time-lapse recordings showed that the labeled endodermal cells passed over the posterior lip of the descending AIP and into the foregut as the LHP folded to form a tube, showing that folding of the endoderm and heart mesoderm occur in parallel in this region (Fig. 5A, Movie 7). To better visualize and localize the dye stream, we amplified its signal immunohistochemically. Doing so highlighted the labeled streams extending anteroposteriorly in the foregut tube (Fig. 5Bb′, white arrow) and confirmed the endodermal/foregut identity of these cells (Fig. 5Bb″, arrow). It also showed that they originated from cells along the transverse extent of the mediolateral stripes made in the heart primordia (Fig. 5Ba, arrowhead). This finding revealed similarities between heart tube and foregut formation: (1) mediolateral orientation in these flat primordia (the heart mesoderm and overlying endoderm) is converted to anteroposterior orientation in the tubular heart and foregut; (2) anteroposterior orientation in both flat primordia is converted to mediolateral orientation; and (3) both primordia undergo oriented extension along the elongating axis of the heart tube and foregut. Additionally, the posterior ends of labeled cell streams in the foregut and heart tubes overlapped (Figs 3Bh and 5Bb′, black arrows), further suggesting that tissues elongated posteriorly in concert. Collectively, these findings suggest that the foregut and heart tube coordinately form, through similar tissue movements (Fig. 5C), and elongate posteriorly together, not just by the progression of tube formation from their flat primordia, but also by oriented tissue extension.

Directional extension of endoderm is likely myosin dependent

We next examined p-myoII localization in the endoderm to determine whether oriented extension of the endoderm (Fig. 5B), like that of the heart mesoderm, is myosin dependent. Immunofluorescence revealed abundant and planar-polarized distribution of p-myoII in both the foregut and contiguous endoderm surrounding the AIP (Fig. 6A-D′). In the elongating foregut, p-myoII supracellular cables were aligned along the mediolateral axis (Fig. 6A,C,C′), in accordance with the

Development (2018) 145, dev152488. doi:10.1242/dev.152488

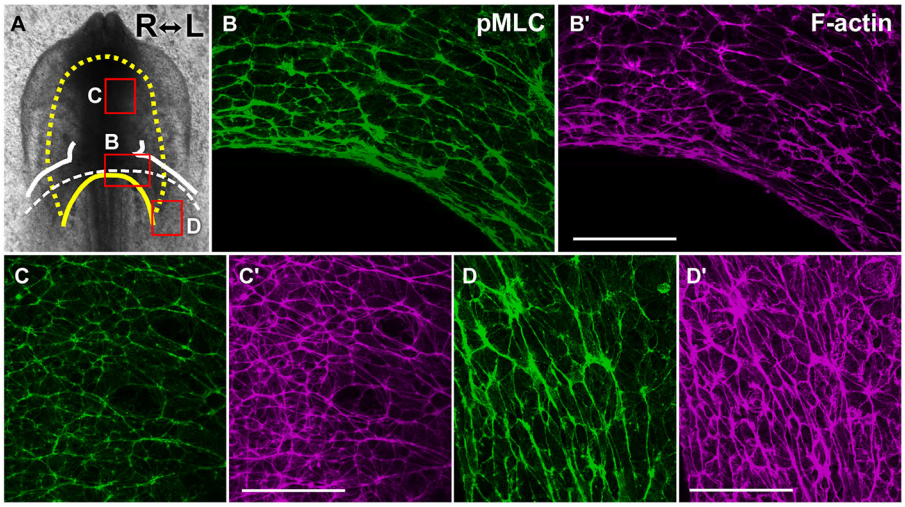

Fig. 6. Phosphorylated-myosin is abundantly localized in a planar polarized pattern in the foregut endoderm. (A) Boxes indicate approximate areas shown in B-D′. The yellow dashed line and solid yellow line delineate the foregut and AIP, respectively. White solid lines outline the primitive heart. A white dashed line depicts the folding edge of lateral heart primordia (LHP). (B,C,D) Immunofluorescence for pMLC in normal embryos at stage 9– (6-somites, 3D projections of confocal *z* stacks). (B′,C′,D′) F-actin (magenta) was counterstained with fluorescent phalloidin. Phosphorylated myosin (p-myoII) was enriched in cell junctions aligned mediolaterally in the foregut (C,C′). Robust p-myoII cables were oriented circumferentially near the AIP (B,B′) and at more-posterior regions (D,D′) where the endoderm overlies the heart primordia before folding. Scale bars: 50 µm.

idea that these cells undergo mediolateral intercalation to lengthen the foregut. Around the AIP, endodermal cells were circumferentially elongated, and robust p-myoII cables were oriented along the edge of the AIP (Fig. 6A,B,B′), consistent with the previous finding that AIP convergence is driven by actomyosin contraction (Varner and Taber, 2012). p-myoII was also abundantly present in the endoderm overlying the heart primordia before folding (Fig. 6A,D,D′), which moved in concert with LHP folding (Fig. 5A). The intense immunofluorescence signal of activated-myosin and its polarized localization (Fig. 6A-D′) suggest that strong contractile forces exist in the foregut endoderm, presumably driving endodermal extension (Fig. 5B) through CE, thereby lengthening the foregut posteriorly.

DISCUSSION

Using cell cluster labeling, we visualized for the first time tissue dynamics during early heart tube formation, discovering that the initially flat heart primordia rapidly remodel into the elongated tube by dramatically changing their overall morphology through CE: they converge toward the midline to form a narrow midline tube, while rapidly extending it perpendicularly. This finding solves the mystery of how the initially narrow mediolateral dimension of the primordia can rapidly generate the long anteroposterior dimension of the heart tube (Fig. 1B). In addition, our data reveal that both the lateral and medial heart fields form the early heart tube by essentially the same mechanism in coordination with neighboring foregut formation. Collectively, our results provide a global picture of heart tube formation and fill the gaps in modern fate maps (Fig. 1B) (Abu-Issa and Kirby, 2008; Cai et al., 2003; Kelly et al., 2001), which are based on extrapolation between stages rather than time-lapse imaging as used here.

The MHP and LHP form the early heart tube in essentially the same way

Although the FHF/LHP have long been known to form the heart tube by ventrally folding and fusing at the midline, how the SHF/MHP incorporate into the heart tube remained unclear (Fig. 1A) (Francou et al., 2014; Sinha et al., 2012, 2015; Uribe et al., 2014). Our cell labeling visualized for the first time the process of early tube formation from both the MHP and LHP, showing that the MHP similarly form the heart tube through ventral folding and fusion as do the LHP (Figs 2, 3 and 7). Because of the difference in their positional relationship with the AIP, the timing of ‘folding’ and ‘fusion’ differ between the MHP and LHP. Folding of the entire heart primordia occurs in concert with AIP descent, progressively from their medial to lateral sides (Fig. 7B,C). Thus, the MHP fold first and the LHP then follow. Both fold diagonally, in the medioposterior direction, thereby reorienting their initial mediolateral polarity to the anteroposterior direction. Although this reorientation by diagonal folding has been proposed previously, our data are the first to demonstrate it and they also suggest that the folding is directed by medial convergence and posteriorward movement of the AIP. As the MHP first fold, this medioposteriorward folding brings the areas near the boundary of the MHP and LHP into the midline for initial fusion (Fig. 7Ba-c,Ca-c, blue arrow). Subsequently, as the AIP moves further posteriorly, the LHP likewise fold medioposteriorly while fusing toward the midline, forming the posterior heart tube (Fig. 7Bc, d,Cc,d). Concomitantly, the MHP, which have already completed folding at this time, also fuse toward the midline to form the anterior heart tube (Fig. 7Ac,d,Bc,d,Cc,d). Thus, the MHP first fold then fuse toward the midline progressively in the anterior direction, whereas the LHP fold concomitantly with fusion to form more posterior levels of the heart tube, elongating the heart tube bidirectionally (Fig. 7Cc,d, gray arrows) (Moreno-Rodriguez et al., 2006).

Directional cell rearrangement drives heart tube elongation

We show that both the LHP and MHP undergo CE. Labeling cells in adjacent regions with different colors demonstrated that heart mesodermal cells undergo intercalation perpendicularly to the direction of tissue extension (Fig. 4A). Phosphorylated myosin was enriched at cell junctions along the convergence axis (Fig. 4B), and its inactivation markedly impaired tissue extension, resulting in severe inhibition of heart lengthening (Fig. 4C, Fig. S6). Collectively, these results strongly suggest that heart tube elongation is driven in large part by myosin-dependent directional cell rearrangement. Although the early heart tube has been considered to lengthen by progressive cell addition (increase in cell number), we propose here that reorganization of cells is a key mechanism for rapid elongation.

One may wonder whether compromised heart extension after Y27632 exposure was indirectly caused via AIP defects, as actomyosin contraction along the AIP was suggested to support heart lengthening (Hosseini et al., 2017). Although the AIP stopped converging and relaxed immediately after Y27632 exposure, it resumed converging/descending within 2 h (Movie 6). Nevertheless, the labeled cell clusters in the heart mesoderm showed almost no extension throughout the recording. This suggests that CE/directional rearrangement of heart cells requires

Development (2018) 145, dev152488. doi:10.1242/dev.152488

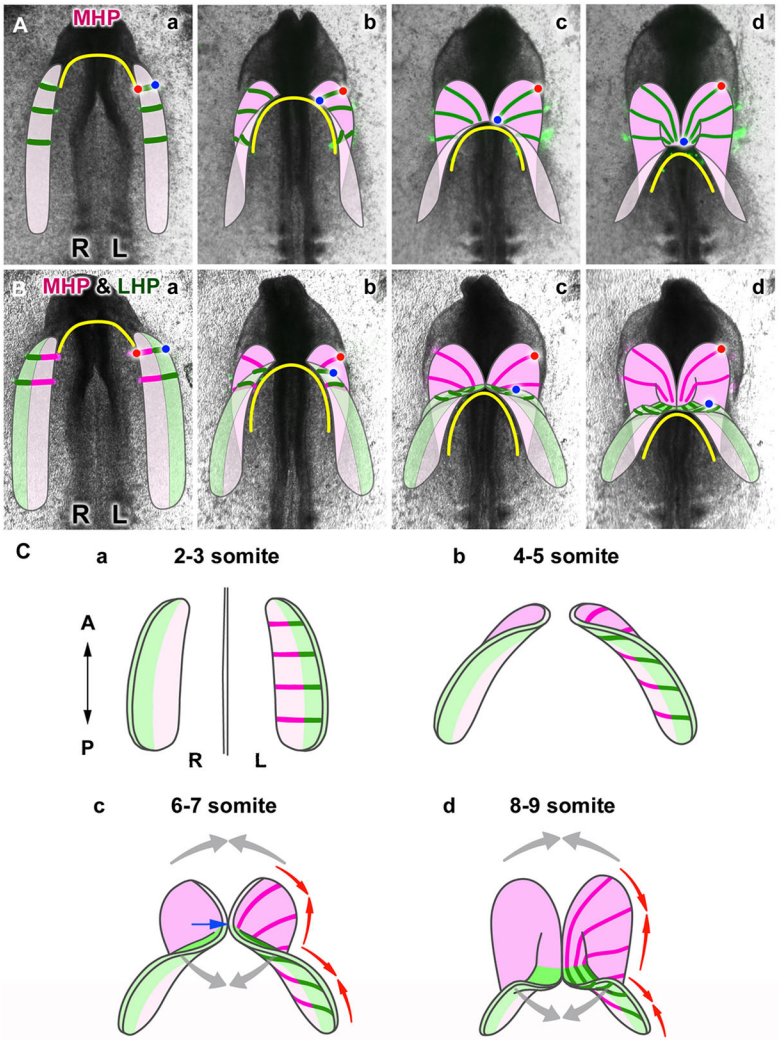

Fig. 7. Tissue dynamics of the heart primordia during formation of the heart tube. (A) Schematic representation of heart tube formation from the medial heart primordia (MHP, pink), based on the cell labeling shown in Fig. 2. The DiO-labeled cell streams are drawn with green lines. Red and blue dots depict the original medial and lateral edges of the MHP, respectively. (B) Schematic representation of tube formation from the MHP (pink) and LHP (the lateral heart primordia; green), based on observations shown in Fig. 3. Magenta and green lines represent DiI- and DiO-labeled cell streams, respectively. Red and blue dots depict the original medial and lateral edges of the entire (MHP+LHP) heart primordium. (C) Diagrams showing the process of early heart tube formation. The paired heart primordia progressively fold, diagonally from their medial (MHP, pink) to lateral (LHP, green) sides. The first fusion of the paired primordia occurs near the boundary between the MHP and LHP (c, blue arrow), and proceeds bidirectionally (gray arrows). Whereas the MHP (pink) complete folding prior to their fusion, the folding and fusion of the LHP occur simultaneously. Both the MHP and LHP converge along the original AP axis (red arrows) as they form the heart tube while extending perpendicularly. In all drawings in A-C, the original ventral and dorsal sides of the primordia are shown in different shades of the same color to indicate how the primordia flip/fold.

heart cell-autonomous myosin contraction, and that this failed to resume after Y27632 exposure, unlike endodermal myosin contraction. In agreement with this, polarized localization of p-myoII in the heart mesoderm was abolished after Y27632 exposure (Fig. 4Bc,c′), whereas p-myoII still remained in the endoderm (not shown), probably because of its high abundancy in this layer (Fig. 6). Additionally, heart extension is not entirely dependent on endodermal movements because labeled cell clusters in the heart mesoderm extended more than the ones in the endoderm, as discussed below. Therefore, although endodermal defects may be partly responsible for the failed heart extension, it is likely that the inhibitor also had a direct effect on heart cells.

In addition to cell rearrangement, hypertrophy and differential proliferation likely shape the early heart tube (Hosseini et al., 2017; Shi et al., 2014). In our confocal imaging, heart cells seemed to enlarge during heart tube formation (Fig. 4A), but this growth did not occur preferentially along the tissue extension axis; rather, cells were elongated perpendicularly to it. Thus, although hypertrophy may contribute to heart lengthening, it is unlikely to be its major driver.

Convergence drives formation of the midline heart tube

Our data show that convergence occurs in the initially long anterior-posterior dimension of the bilateral heart primordia to form the narrow, tubular heart (Figs 2 and 3, note that the initial anteroposterior axis converts to the mediolateral axis). Thus, CE not only extends the heart tube, it also remodels the flat primordia into a midline tube by converging them toward the midline. This tube formation through convergence also explains how SHF cells are deployed into the heart poles during early heart tube formation. The SHF/medial region of the bilateral heart primordia (MHP) is displaced dorsally and anteriorly during heart tube formation (Kelly et al., 2001) and comes to lie dorsal to the initial heart tube. Our data show that this flat, MHP-derived dorsal heart mesoderm converges toward the midline, as do other parts of the heart primordia, forming the anterior pole of the heart tube (Fig. 2F-J and 7A-C). That is, deployment through convergence is not unique to the MHP/SHF, but occurs in the entire heart primordium as a part of the global process of early heart tube formation. Although incorporation of SHF cells continues at least until HH stage 22 (de la Cruz et al., 1977), our study only addresses stages up to HH12. Thus, whether SHF deployment at later stages occurs similarly needs to be examined in future studies. At the end time-point of our movies, some MHP-derived labeled cells remained in the dorsal heart mesoderm in continuity with the labeled cell stripes within the anterior heart tube (Figs 2J′ and 3Ah, arrowheads). We speculate that these cells subsequently incorporate into the anterior pole similarly to that observed at earlier stages. Because breakdown of the dorsal mesocardium occurs from the mid-level of the heart tube and proceeds bidirectionally, MHP cells must enter the heart tube

Development (2018) 145, dev152488. doi:10.1242/dev.152488

solely from its poles after this breakdown occurs (Linask et al., 2005; Patten, 1922), whereas, at earlier stages, MHP cells incorporate both from the nascent poles and the dorsal side of the initial heart tube. Because the AIP progressively moves posteriorly away from the anterior pole, later incorporation is likely independent of AIP movements. The newly formed foregut, underlying the dorsal heart mesoderm, seemingly undergoes CE, driven by myosin contraction (Fig. 6C,C′), to lengthen while narrowing. Thus, the later incorporation of MHP might be either supported by CE of the foregut, or independent of endodermal morphogenesis.

Mouse mutants of non-canonical Wnt/planar cell polarity (PCP) pathway components display a shortened outflow tract (OFT) (Sinha et al., 2012, 2015). This shortening is attributed to defective SHF deployment, and the Wnt/PCP pathway has been proposed to regulate radial cell intercalation to convert multi-layered SHF progenitors into a single-layered sheet, thereby promoting SHF deployment. By contrast, our data show that MHP/SHF cells undergo mediolateral intercalation. Moreover, given our finding that the heart tube lengthens by a directional tissue extension, both defective extension and deployment of the primordia, which are mediated by mediolateral intercalation, may also be the cause of OFT shortening in PCP mutants (Iizuka-Kogo et al., 2015). Taken together, CE likely plays key roles in lengthening of the heart tube by driving directional tissue extension, as well as progressive incorporation of progenitors.

The heart tube and foregut coordinately form through similar tissue dynamics

Our cell labeling reveals that the endoderm forms the foregut through previously unrecognized movements: the endoderm overlying the bilateral heart primordia converges toward the embryonic midline while diagonally folding and thereby reorienting their mediolateral axis anteroposteriorly (Fig. 5C). This endodermal movement is quite similar to that of the heart primordia during heart tube formation (Figs 5C and 7). Our cell labeling further demonstrates that these two layers move in concert (Fig. 5A) (Aleksandrova et al., 2015). In addition, our data suggest that, similarly to the heart tube, the foregut lengthens by CE, in agreement with the presumption of Stalsberg and DeHaan (1968). CE of the foregut seems to be driven by myosin-dependent mediolateral cell intercalation, as cells labeled with dyes extend similarly to those in the heart (Fig. 5B) and p-myoII supracellular cables are aligned perpendicularly to the direction of foregut extension (Fig. 6C,C′). Together, our findings suggest that the heart tube forms and elongates through tissue movements that are coordinated with those of the foregut endoderm.

Does foregut formation play a role in heart tube elongation?

Although this question has not been answered directly, our observations that the heart mesoderm directionally extended synchronously with AIP movements suggest that endodermal mechanical forces may facilitate heart extension by guiding the directional rearrangement of heart cells. External forces exerted by neighboring morphogenetic movements orient cell behaviors that drive directional tissue extension in several models (Aigouy et al., 2010; Imuta et al., 2014; Lye et al., 2015). The endoderm and heart mesoderm are in close contact during heart tube formation (Linask and Lash, 1986; Varner and Taber, 2012), and the foregut endoderm likely possesses strong contractile forces, as evidenced by abundant and polarized localization of phosphorylated myosin (Fig. 6). Moreover, using computational modeling, Hosseini and coworkers (2017) showed that actomyosin contraction along the AIP generates posteriorward tension. Although was not experimentally tested, they proposed a model in which tension pulls and stretches the heart tube posteriorly, assisting in its elongation. Our cell cluster labeling showed that the heart primordia actually extend medial-posteriorly coordinately with AIP convergence and descent (Figs 2 and 3), rather than just posteriorly, as they proposed, but otherwise our results support their model. Taken together, endodermal contraction and resulting foregut extension may physically pull and stretch the heart mesoderm to trigger directional cell intercalation, stimulating CE of the heart. However, the possibility that the foregut serves as a scaffold for heart tube extension cannot be excluded.

Heart tube extension is likely to be at least partially independent of foregut formation. Our cell cluster labeling shows that heart mesoderm undergoes more extension than does the endoderm (Figs 3Bh and 5B, approximately 1.5-2 times greater). While rapidly elongating, the heart tube undergoes rightward looping, whereas the foregut elongates along the midline axis. Considering that heart looping requires more rapid elongation than that occurring in the adjacent foregut, left-right asymmetry in autonomous heart-mesoderm extension might be key for looping. More specifically, left heart cells may more actively rearrange than do right cells, driving asymmetric heart elongation and looping.

In conclusion, we have discovered mechanisms that drive dynamic morphological changes and rapid lengthening of the early heart primordia in coordination with neighboring foregut morphogenesis. Based on previously published studies and our current results, it seems likely that both endodermal forces and autonomous heart mesodermal forces play important roles in heart tube extension, but further experimental studies are required to resolve the exact roles of these tissues in heart tube formation and extension.

MATERIALS AND METHODS

Embryo preparation and culture

Fertilized White Leghorn chicken eggs were incubated at 38.5°C until embryos reached stage 7/7+ (1-2 somites) (Hamburger and Hamilton, 1992). Whole embryos were removed from eggs using filter paper rings and placed ventral-side up on 35 mm plastic culture dishes containing agarose-albumen medium (0.2% agarose, 50% albumen, 50% saline: 123 mM NaCl in H_2O; modified from Chapman et al., 2001). Embryos were gently washed with chick saline (123 mM NaCl/H_2O) to remove yolk on their surface and cultured at 38.5°C in a humid chamber. All protocols using chick embryos were approved by the University of Utah Institutional Animal Care and Use Committee (IACUC, protocol 16-12018).

Cell labeling and time-lapse imaging

DiI [1,1′-dioctadecyl-3,3,3′,3′-tetramethylindocarbocyanine perchlorate; Molecular Probes, D282; 0.125% in 1:40 DMF (*N*,*N*-dimethylformamide): tetraglycol] or DiO (3,3′-dioctadecyloxacarbocyanine perchlorate; Molecular Probes, D275; 0.5% in 1:20 DMF:tetraglycol) solution was injected into the heart mesoderm at the two- to three-somite stage from its ventral side using fine pulled glass micropipettes, a microinjector (Picospritzer II; General Valve) and a micromanipulator (Narishige). Labeled embryos were subjected to time-lapse recording at 38.5°C in a heated chamber until embryos reached around the 15-16 somite stage. Images were acquired with 15 min time-intervals, six or seven *z*-steps for each time-point, using a Leica M205 FA automated fluorescence stereomicroscope, a DFC 345Fx monochrome camera and LAS AF software. Images at optimal focus were selected from the *z*-series for each time-point and aligned along the time-series using the Stackreg plugin of ImageJ to make time-lapse movies. At least 20 embryos were successfully labeled for time-lapse imaging in the LHP and/or MHP during heart tube formation (Figs 2 and 3), and consistent results were obtained from embryo to embryo in each labeled region.

Development (2018) 145, dev152488. doi:10.1242/dev.152488

For fixation and amplification of dye-labeled cells in whole mounts and tissue sections, mixtures of DiI and CRSE (Rhodamine: 5-carboxytetramethylrhodamine, succinimidyl ester, Molecular Probes, C2211) or DiO and CFSE [Fluorescein: 5-(and-6)-carboxyfluorescein diacetate, succinimidyl ester, Molecular Probes, C1157] were injected. Embryos were processed for whole-mount immunostaining using anti-rhodamine rabbit IgG polyclonal antibody (Molecular Probes, A-6397) and alkaline phosphatase (AP)-conjugated anti-fluorescein antibody (Roche, 11 426 338 910), as described previously (Lopez-Sanchez et al., 2004). For the secondary antibody, horseradish peroxidase (HRP)-conjugated goat anti-rabbit IgG (Jackson ImmunoResearch) was used. Embryos were stained with NBT/BCIP and DAB substrates to detect AP and HRP activity, respectively. Selected samples were embedded in paraffin wax and serially sectioned using standard techniques.

Confocal imaging of labeled cells

Cell clusters in the heart mesoderm were labeled with DiI or DiO and immediately imaged using a Leica SP5 laser-scanning microscope with a 20× objective. Embryos were then returned to culture and fixed at stage 11/11+ (13-14 somites) with 4% PFA/PBS (phosphate-buffered saline), incubated with To-pro-3 Iodide (Molecular Probes, T3605) for nuclear staining, cleared through a graded series of glycerol/PBS and reimaged in 90% glycerol/H_2O using a Leica SP5 with 20× and 40× objectives. Data sets were volume rendered and fluorescent signals in the myocardial layer were extracted using FluoRender software.

Whole-mount immunofluorescence

Embryos were fixed with 4% PFA/PBS for 15 min at room temperature. Embryos were then rinsed with PBS, incubated with 3% BSA/TBSTx (Tris-buffred saline containing 0.1% triton X-100) for 30 min on ice, followed by overnight incubation at 4°C with anti-phospho-myosin light chain 2 (pMLC, Ser19, Cell Signaling Technologies, 3675) at 1:50 dilution in Can Get Signal immunostain solution B (TOYOBO) containing 0.1% triton X-100. After extensive washing, embryos were incubated overnight with Alexa 488-conjugated secondary antibodies (1:200 dilution) and Alexa 647-conjugated phalloidin (1:100) at 4°C. After extensive washing, embryos were cleared through a graded series of glycerol/TBS and imaged in 80% glycerol/H_2O with a Leica SP6 confocal microscope. Fluorescent signals in the outer surface of the heart tube or the heart mesoderm were extracted from image stacks using FluoRender software. 3D rendering was created from each extracted image stack using the 3D Project function of ImageJ.

Quantification of the orientation of phosphorylated-myosin II (p-myoII) supracellular cables

p-myoII cables were visualized by whole-mount immunofluorescence of pMLC and confocal microscopy, and 3D projections of the confocal *z*-stacks were created as described above. To eliminate noise, high-contrast images were generated by changing the brightness and contrast to the range of 35-151 (originally 0-225) with ImageJ. Three images were chosen from different embryos, including the one shown in Fig. 4Bb-b', for measurements. Using the line tool of ImageJ, the lengths and angles (0°-180°) of p-myoII fibers in an area (442 × 496 pixels^2) of the dorsal heart mesoderm corresponding to the region shown in Fig. 4Bb were measured. The data were plotted using Excel Scatter XY chart, where angles and lengths of fibers were shown in the *x* and *y* axes, respectively.

Pharmaceutical treatment

Whole embryos were harvested using filter paper rings, and the heart mesoderm was labeled with DiI at stage 7+ (2 somites) as described above. When embryos reached stage 8/9− (4-6 somites), they were transferred to 35 mm dishes containing 2 ml of solid agarose-albumen medium pretreated with 60-120 µl of 200 µM Y27632 or chick saline (controls). An additional 60-100 µl of 200 µM Y27632 or saline was gently dropped onto the embryos, which were then cultured at 38°C with time-lapse recording. For each experiment, a fresh solution of 200 µM Y27632 (Abcam, ab120129) was prepared by diluting 50 mM Y27632/H_2O stock solution with chick saline (123 mM NaCl in H_2O).

To evaluate the effect of Y27632 treatment on non-muscle myosin II, non-DiI labeled embryos were treated with Y27632, using the same procedure, from stage 8+/9− (5-6 somites). Embryos were fixed at stage 9−/9+ (6-8 somites) and processed for whole-mount immunofluorescence using anti-pMLC antibody as described above.

Acknowledgements

We thank Kristen Kwan (University of Utah), Anne Moon (Weis Center for Research, Geisinger Clinic) and Yusuke Watanabe (National Cerebral and Cardiovascular Center Research Institute) for critical reading of the manuscript and helpful discussions.

Competing interests

The authors declare no competing or financial interests.

Author contributions

Conceptualization: H.K., Y.S.; Methodology: G.C.S., Y.S.; Validation: H.K.; Formal analysis: H.K.; Investigation: H.K.; Resources: S.Y.-T., K.T., G.C.S., Y.S.; Data curation: H.K.; Writing - original draft: H.K.; Writing - review & editing: H.K., S.Y.-T., K.T., G.C.S., Y.S.; Visualization: Y.S.; Supervision: Y.S.; Project administration: Y.S.; Funding acquisition: Y.S.

Funding

This work was supported by the March of Dimes Foundation and by the National Institutes of Health [the Eunice Kennedy Shriver National Institute of Child Health and Human Development (R01 HD066121) and the National Heart, Lung, and Blood Institute, Programs of Excellence in Glycosciences (P01 HL107152) to Y.S.]. The content is solely the responsibility of the authors and does not necessarily represent the official views of the funding agencies. Deposited in PMC for release after 12 months.

Supplementary information

Supplementary information available online at
http://dev.biologists.org/lookup/doi/10.1242/dev.152488.supplemental

References

Abu-Issa, R. and Kirby, M. L. (2007). Heart field: from mesoderm to heart tube. *Annu. Rev. Cell Dev. Biol.* **23**, 45-68.

Abu-Issa, R. and Kirby, M. L. (2008). Patterning of the heart field in the chick. *Dev. Biol.* **319**, 223-233.

Aigouy, B., Farhadifar, R., Staple, D. B., Sagner, A., Röper, J.-C., Jülicher, F. and Eaton, S. (2010). Cell flow reorients the axis of planar polarity in the wing epithelium of Drosophila. *Cell* **142**, 773-786.

Aleksandrova, A., Czirok, A., Kosa, E., Galkin, O., Cheuvront, T. J. and Rongish, B. J. (2015). The endoderm and myocardium join forces to drive early heart tube assembly. *Dev. Biol.* **404**, 40-54.

Bertet, C., Sulak, L. and Lecuit, T. (2004). Myosin-dependent junction remodelling controls planar cell intercalation and axis elongation. *Nature* **429**, 667-671.

Buckingham, M., Meilhac, S. and Zaffran, S. (2005). Building the mammalian heart from two sources of myocardial cells. *Nat. Rev. Genet.* **6**, 826-835.

Cai, C. L., Liang, X., Shi, Y., Chu, P.-H., Pfaff, S. L., Chen, J. and Evans, S. (2003). Isl1 identifies a cardiac progenitor population that proliferates prior to differentiation and contributes a majority of cells to the heart. *Dev. Cell* **5**, 877-889.

Chapman, S. C., Collignon, J., Schoenwolf, G. C. and Lumsden, A. (2001). Improved method for chick whole-embryo culture using a filter paper carrier. *Dev. Dyn.* **220**, 284-289.

DeHaan, R. L. (1965). Development of pacemaker tissue in the embryonic heart. *Ann. N. Y. Acad. Sci.* **127**, 7-18.

de la Cruz, M. V., Sánchez Gómez, C., Arteaga, M. M. and Argüello, C. (1977). Experimental study of the development of the truncus and the conus in the chick embryo. *J. Anat.* **123**, 661-686.

Francou, A., Saint-Michel, E., Mesbah, K. and Kelly, R. G. (2014). TBX1 regulates epithelial polarity and dynamic basal filopodia in the second heart field. *Development* **141**, 4320-4331.

Hamburger, V. and Hamilton, H. L. (1992). A series of normal stages in the development of the chick embryo. 1951. *Dev. Dyn.* **195**, 231-272.

Harvey, R. P. (1998). Cardiac looping–an uneasy deal with laterality. *Semin. Cell Dev. Biol.* **9**, 101-108.

Hosseini, H. S., Garcia, K. E. and Taber, L. A. (2017). A new hypothesis for foregut and heart tube formation based on differential growth and actomyosin contraction. *Development* **144**, 2381-2391.

Iizuka-Kogo, A., Senda, T., Akiyama, T., Shimomura, A., Nomura, R., Hasegawa, Y., Yamamura, K. I., Kogo, H., Sawai, N. and Matsuzaki, T. (2015). Requirement of DLG1 for cardiovascular development and tissue elongation during cochlear, enteric, and skeletal development: Possible role in convergent extension. *PLoS ONE* **10**, e0123965.

Imuta, Y., Koyama, H., Shi, D., Eiraku, M., Fujimori, T. and Sasaki, H. (2014). Mechanical control of notochord morphogenesis by extra-embryonic tissues in mouse embryos. *Mech. Dev.* **132**, 44-58.
Kasza, K. E. and Zallen, J. A. (2011). Dynamics and regulation of contractile actin–myosin networks in morphogenesis. *Curr. Opin. Cell Biol.* **23**, 30-38.
Kelly, R. G. and Buckingham, M. E. (2002). The anterior heart-forming field: Voyage to the arterial pole of the heart. *Trends Genet.* **18**, 210-216.
Kelly, R. G., Brown, N. A. and Buckingham, M. E. (2001). The arterial pole of the mouse heart forms from Fgf10-expressing cells in pharyngeal mesoderm. *Dev. Cell* **1**, 435-440.
Linask, K. K. and Lash, J. W. (1986). Precardiac cell migration: fibronectin localization at mesoderm-endoderm interface during directional movement. *Dev. Biol.* **114**, 87-101.
Linask, K. K., Han, M., Cai, D. H., Brauer, P. R. and Maisastry, S. M. (2005). Cardiac morphogenesis: matrix metalloproteinase coordination of cellular mechanisms underlying heart tube formation and directionality of looping. *Dev. Dyn.* **233**, 739-753.
Lopez-Sanchez, C., Garcia-Martinez, V., Lawson, A., Chapman, S. C. and Schoenwolf, G. C. (2004). Rapid triple-labeling method combining in situ hybridization and double immunocytochemistry. *Dev. Dyn.* **230**, 309-315.
Lye, C. M., Blanchard, G. B., Naylor, H. W., Muresan, L., Huisken, J., Adams, R. J. and Sanson, B. (2015). Mechanical coupling between endoderm invagination and axis extension in Drosophila. *PLoS Biol.* **13**, e1002292.
Lyons, I., Parsons, L. M., Hartley, L., Li, R., Andrews, J. E., Robb, L. and Harvey, R. P. (1995). Myogenic and morphogenetic defects in the heart tubes of murine embryos lacking the homeo box gene Nkx2-5. *Genes Dev.* **9**, 1654-1666.
Ma, X. and Adelstein, R. S. (2012). In vivo studies on nonmuscle myosin II expression and function in heart development. *Front. Biosci.* **17**, 545-555.
Männer, J. (2000). Cardiac looping in the chick embryo: a morphological review with special reference to terminological and biomechanical aspects of the looping process. *Anat. Rec.* **259**, 248-262.
Männer, J. (2009). The anatomy of cardiac looping: a step towards the understanding of the morphogenesis of several forms of congenital cardiac malformations. *Clin. Anat.* **22**, 21-35.
Moreno-Rodriguez, R. A., Krug, E. L., Reyes, L., Villavicencio, L., Mjaatvedt, C. H. and Markwald, R. R. (2006). Bidirectional fusion of the heart-forming fields in the developing chick embryo. *Dev. Dyn.* **235**, 191-202.
Nishimura, T., Honda, H. and Takeichi, M. (2012). Planar cell polarity links axes of spatial dynamics in neural-tube closure. *Cell* **149**, 1084-1097.
Patten, B. M. (1922). The formation of the cardiac loop in the chick. *Am. J. Anat.* **30**, 373-397.
Rozbicki, E., Chuai, M., Karjalainen, A. I., Song, F., Sang, H. M., Martin, R., Knölker, H.-J., MacDonald, M. P. and Weijer, C. J. (2015). Myosin-II-mediated cell shape changes and cell intercalation contribute to primitive streak formation. *Nat. Cell Biol.* **17**, 397-408.
Shi, Y., Yao, J., Xu, G. and Taber, L. A. (2014). Bending of the looping heart: differential growth revisited. *J. Biomech. Eng.* **136**, 81002.
Sinha, T., Wang, B., Evans, S., Wynshaw-Boris, A. and Wang, J. (2012). Disheveled mediated planar cell polarity signaling is required in the second heart field lineage for outflow tract morphogenesis. *Dev. Biol.* **370**, 135-144.
Sinha, T., Li, D., Théveniau-Ruissy, M., Hutson, M. R., Kelly, R. G. and Wang, J. (2015). Loss of Wnt5a disrupts second heart field cell deployment and may contribute to OFT malformations in DiGeorge syndrome. *Hum. Mol. Genet.* **24**, 1704-1716.
Stalsberg, H. and DeHaan, R. L. (1968). Endodermal movements during foregut formation in the chick embryo. *Dev. Biol.* **18**, 198-215.
Tanaka, M., Chen, Z., Bartunkova, S., Yamasaki, N. and Izumo, S. (1999). The cardiac homeobox gene Csx/Nkx2.5 lies genetically upstream of multiple genes essential for heart development. *Development* **126**, 1269-1280.
Uribe, V., Badía-Careaga, C., Casanova, J. C., Domínguez, J. N., de la Pompa, J. L. and Sanz-Ezquerro, J. J. (2014). Arid3b is essential for second heart field cell deployment and heart patterning. *Development* **141**, 4168-4181.
Varner, V. D. and Taber, L. A. (2012). Not just inductive: a crucial mechanical role for the endoderm during heart tube assembly. *Development* **139**, 1680-1690.
Ye, D., Xie, H., Hu, B. and Lin, F. (2015). Endoderm convergence controls subduction of the myocardial precursors during heart-tube formation. **142**, 2928-2940.
Zallen, J. A. and Wieschaus, E. (2004). Patterned gene expression directs bipolar planar polarity in Drosophila. *Dev. Cell* **6**, 343-355.